Eur. J. Wood Prod. (2018) 76:201–212
DOI 10.1007/s00107-017-1221-8

ORIGINAL

Timber steel-fibre-reinforced concrete floor slabs subjected to fire

Jan Ekr[1] · Eva Caldova[2] · Petr Vymlatil[3] · Frantisek Wald[2] · Anna Kuklikova[2]

Received: 8 December 2015 / Published online: 18 July 2017

Abstract This paper presents a finite element model (FE model) for a numerical analysis of a composite steel-fibre-reinforced concrete (SFRC) slab with unprotected secondary timber beams subjected to fire, taking tensile membrane action into account. The material models were calibrated by material tests and push-out tests in a preliminary study, and then the FE model was validated against the results of a full-scale furnace test. The validated FE model takes into account geometric and material nonlinearity, mechanical damage due to thermal loading, and the non-linear connection between the SFRC slab and the timber beams. A new material model was created to improve the simulated behaviour of the SFRC, especially in tension. The validated FE model was supplemented by a semi-probabilistic safety concept based on the Eurocode standards, and was applied to define the fire resistance of different variants of timber SFRC flooring subjected to fire with various slab dimensions and design loads. This approach will be used to create a catalogue in which the fire resistance will be defined for specific parameters of the structure, for example dimensions, loads and materials. The research presented in this paper follows up on a previous study, which was presented in 2014.

✉ Jan Ekr
ekr.j@fce.vutbr.cz

[1] Faculty of Civil Engineering, Brno University of Technology, Veveri 95, 602 00 Brno, Czech Republic

[2] Faculty of Civil Engineering, Czech Technical University in Prague, Thakurova 7, 166 29 Prague 6, Czech Republic

[3] Designtec s.r.o., Uhelna 1186/8, 779 00 Olomouc, Czech Republic

1 Introduction

Timber–concrete composite structures are currently used especially in reconstructing and constructing prefabricated residential houses. In a concrete slab that forms a part of a timber–concrete composite floor, a reinforcement is designed for the restrain caused by concrete shrinkage, and to obtain sufficient resistance to the tensile forces around the shear connectors. The slab needs to be at least 60 mm in thickness, due to the amount of reinforcement, its location usually in the middle of the slab, and also the lap splices and the concrete cover of the reinforcement (min. 20 mm). This seriously increases the dead-load of a composite floor (Holschemacher et al. 2002). Several studies on new timber–concrete composite floors have been conducted in recent decades, for example, Ceccotti (2002) and Stojić and Cvetković (2001). Studies taking into account fire situations have also been made (e.g., Fontana and Frangi 2000; Frangi et al. 2009). In certain cases, the usual reinforced concrete may be replaced by a Steel Fibre Reinforced Concrete (SFRC) mixture. This innovative structural mixture with specific hardened concrete properties was developed to reduce slab thickness, and it offers several advantages. For example, experimental and theoretical studies show that the presence of steel fibres may increase the ultimate strain and improve the ductility of fibre-reinforced concrete elements (Lie and Kodur 1996). This was proven by Bednar et al. (2012) for Arcelor HE 75/50 steel fibres using 70 kg per cubic meter of concrete. In addition, concrete elements with dispersed steel fibres have lower creep and shrinkage than classical reinforced concrete elements. Quicker, more efficient installation without armouring might reduce the entry costs of SFRC construction. Experimental studies have also shown that the compressive strength at elevated temperatures of fibre-reinforced concrete is higher than the

compressive strength of plain concrete. Overall, at elevated temperatures, fibre-reinforced concrete exhibits mechanical properties that are more beneficial to fire resistance than those of plain concrete (Lie and Kodur 1996). Due to the ductile post-crack behaviour of SFRC, the remaining tension strength can be used for design purposes. Steel fibres can therefore partly or fully replace conventional reinforcement (Holschemacher et al. 2002).

The behaviour of a heated slab depends on its embedment in the surrounding structure. Recently, fires in buildings and full-scale fire tests in the UK have shown that slabs supported on four sides have much higher fire resistance than slabs supported at two ends. This is due to two-way action and tensile membrane action (Lim 2003). At ambient temperature, the composite timber-SFRC slab transfers the loads by bending. During fire conditions, secondary timber beams lose strength, leading to large deflections of the SFRC slab and the activation of membrane forces (Bailey 2004). This phenomenon results in increased load bearing capacity even with unprotected secondary beams. The increased load bearing capacity of slabs supported on four sides has attracted a great deal of interest in the steel industry around the world, but the timber industry has not studied the topic to any great extent, and has not published any literature on it.

Within the framework of research performed at the Czech Technical University in Prague, numerical and analytical models are being developed in parallel, aiming to simulate the behaviour of the type of structure described here, when it is exposed to fire. Various independent methods and computational software programs have been developed both for numerical models and for analytical models. This helps in analysing various boundary conditions, material properties, the behaviour of the structure, etc., to find a proper balance between simplifications and exact solutions of various effects influencing the behaviour of a slab, whilst producing results comparable with those from full-scale experiments. This kind of research must always include an experimental part.

This paper focuses on a proposed FE model for predicting the fire resistance of floor slabs. This FE model is an improved version of the FE model described in a preliminary study (Caldova et al. 2014a). The earlier model was determined on the basis of current knowledge about steel concrete composite slabs, and was validated in full-scale tests at ambient temperature and also at elevated temperatures. It performed well, and showed satisfactory agreement with measurements. For example, it showed the same failure mechanisms as were observed during full-scale tests. In addition, the developments of the calculated displacements during the fire in the positions of the installed deflectometers were comparable with the measured results. The domains where the cracking occurs were also comparable, and the evolution of the simulated temperature field in the structure during the fire showed good agreement with measurements. However, the model used in the preliminary study (Caldova et al. 2014a) was not capable of predicting the fire resistance of a composite slab, due to the limits of the SFRC material law that was applied, see Sect. 3.2. A new material law has therefore been developed in ANSYS simulation software (2017), and is used in the current FE model for an SFRC slab. This new material model better describes the behaviour of the SFRC, especially in tension, and thus it is able to predict the overall structural behaviour, the time of structural failure and the load bearing capacity of the composite slab.

The FE model with characteristic material properties following the semi-probabilistic safety concept of the Eurocode (EN 1992-1-2 2004; EN 1995-1-2 2004) was derived from the validated FE model and was used for an assessment of the fire resistance of several variants of a composite slab with different dimensions and loads.

2 Experiments

The main part of the experimental program (Caldova et al. 2014a) was focused on full-scale furnace tests of two floor slabs (ELE-1-120/160 and ELE-2-100/160) with a span of 3.0 m by 4.5 m. Both composite timber–concrete floors were composed of an SFRC slab continuously supported by a glulam timber frame and two glulam secondary beams. The timber frame was fire protected by 10 mm thick wood panels, and the secondary beams were left unprotected in both cases. The basic data for both full-scale specimens are summarized as follows:

- cross section of the secondary beams:
  - 120/160 mm (slab ELE-1-120/160)
  - 100/160 mm (slab ELE-2-100/160)
- timber class:
  - GL24h (slab ELE-1-120/160)
  - GL36c (slab ELE-2-100/160)
- fibre content 70 kg/m^3, HE 75/50 Arcelor steel fibres in both slabs
- in both cases, TCC 7.3 × 150 mm connectors were used with screws inclined 45° to the beam axis in two rows; the distance of the screws in one row was 100 mm
- both specimens have an SFRC slab 60 mm in thickness

The bottom surface of the floor was subjected to a standard fire. Structural loading was applied to the specimen during the test. This loading was induced by the weight of two

concrete blocks and represents a uniform load of 1.8 kN/m^2, which is consistent with the loads in a typical office building. Both experimental arrangements are described in detail in Caldova et al. (2014a).

The thermal and mechanical response of the composite slabs during fire was monitored by 27 thermocouples and 13 deflectometers. Thirteen thermocouples were concreted into the composite slab at three separate locations and were positioned either 20 or 40 mm from an unexposed surface or directly on an unexposed surface. Four thermocouples were located on timber beams and ten thermocouples recorded the gas temperature in the furnace below the floor. The deflectometers were placed on the unexposed surface of the slab. Seven deflectometers measured the vertical deflections (see Fig. 1) and six deflectometers measured the horizontal displacements.

For the ELE-1-120/160 test, the standard fire curve lasting for 150 min was followed. After that, the burners were turned off and the furnace was cooled down naturally. In this phase, at time 154 min, the floor slab specimen failed. The ELE-2-100/160 test followed the standard fire curve for 60 min. After that, the burners were turned off and air access to the furnace was prevented. The test results were recorded during this phase to verify the behaviour of the floor slab throughout the fire event.

From the experimental observations, the process leading to the collapse of the structure (ELE-1-120/160) can be briefly described as follows. At the beginning (to about 10 min), the bottom surface is heated to 400 °C and the SFRC slab has the highest thermal gradient. This causes high straining in the slab. The secondary timber beams are not yet damaged by the fire, and they prevent vertical deflection of the SFRC slab. In the next phase, from 10 to about 30 min, the SFRC slab is still supported by the secondary beams and by the timber frame, which are slowly losing their stiffness and their load bearing capacity due to charring. Although the temperature in the SFRC slab is increasing, the thermal strain on the bottom surface is limited due to the non-linearity of the thermal expansion behaviour. Even the decreasing residual load bearing capacity of the secondary beams is therefore able to prevent further deflection. This can be seen as the plateau in the measured deflection curves in Fig. 2. The stiffness of the secondary beams is decreasing further due to charring. This leads to a change in the structural system to a two-way slab supported by a timber frame with relatively high torsional stiffness. Then the first main crack was observed in the longitudinal direction on the longer side of the slab, and a steep increase in deflection occurred at 30 min. During the development of the first main crack in the subsequent minutes, the dead loads cannot act on the structure transferred in a transversal direction. This causes tensile stresses on the shorter side of the slab and a second main crack started to develop at 45 min. A further increase in thermal strain in the middle of the slab, together with thermal damage to the timber and the SFRC, causes deflection of the central part of the slab. The two main cracks continue to develop, and they lose bending stiffness due to softening and thermal degradation. The secondary beams are almost completely burned after 60 min. In the last phase, after 150 min, the central part separated by the main crack starts to act as a membrane. The rest of the structure acts as a stiff composite ring supporting the membrane. The collapse of the slab occurs due to the loss of load bearing capacity in the main crack and in the central part of the slab, and the composite ring is disjoined completely, see Fig. 3.

In addition to the full-scale furnace tests, standard cube compressive tests and four point bending tests of SFRC at

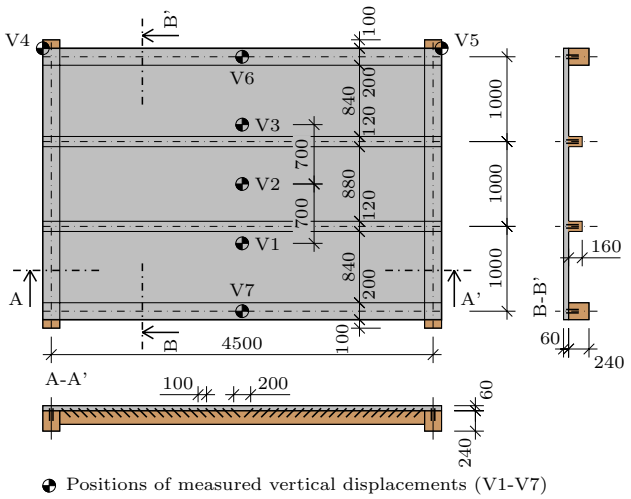

Fig. 1 Dimensions of the specimen (ELE-1-120/160) and positions of the measured vertical displacements

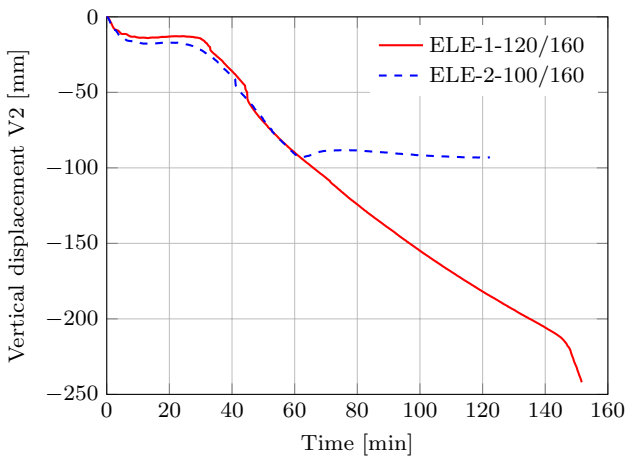

Fig. 2 Vertical displacements in the centre of the timber–concrete composite floors during the fire tests (Caldova et al. 2014a)

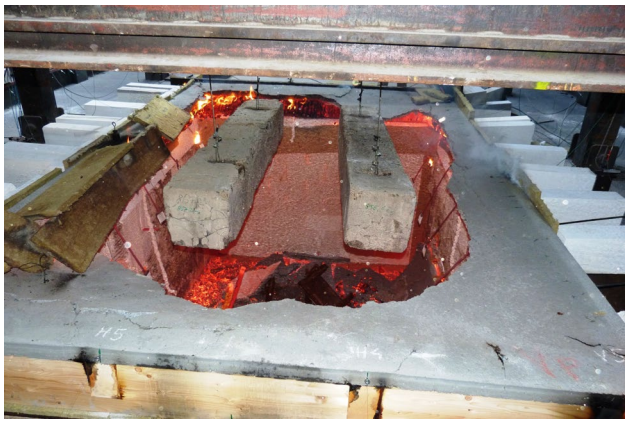

Fig. 3 Collapse of composite floor slab ELE-1-120/160 (Caldova et al. 2014a)

ambient and elevated temperatures were also performed. These tests were for calibrating the material properties for SFRC material law, see Sect. 3.2. To determine the shear bearing capacity and the load-displacement curve of the connection between the timber and the SFRC, a series of shear push-out tests at ambient temperature were also performed (Caldova et al. 2014b). The material properties of model of the connectors were calibrated on the basis of the measured data, see Sect. 3.3.

3 Material models

In nonlinear FEM analyses of structures subjected to fire, material models are essential for predicting the collapse of the structures. Each part of a structure must be represented by an appropriate material law to handle important phenomena such as heat transfer, charring, thermal damage and mechanical damage. The structure presented here consists of timber beams and an SFRC slab coupled with screws. Great importance is given to the material model of SFRC, which is crucial for predicting the collapse of the structure. This is because the unprotected secondary timber beams are already burned before the structure fails, and the load bearing capacity depends only on the SFRC slab, which act as a membrane supported by the timber frame.

3.1 Timber

Timber beams were modelled as transversally isotropic material elements. The elastic material properties of glued laminated timber GL24h were adopted from EN 1995-1-1 (2004). Timber charring was taken into consideration as a factor reducing the elastic moduli and the tensile strength due to temperature change. Relevant functions were taken from EN 1995-1-2 (2004). The coefficient of thermal expansion of timber is about 4.0×10^{-6} °C^{-1} valid from 20 to 300 °C (Frangi and Fontana 2003). For temperatures above 300 °C this coefficient is not meaningful, because the timber is completely charred. Due to the fact that SFCR has a higher coefficient of thermal expansion (12.0×10^{-6} °C^{-1} at 20 °C, and increases up to 700 °C), it is to be expected that the thermal expansion of timber does not influence the behaviour of the slab during the fire test. The thermal expansion of timber was therefore neglected in the material model for timber.

3.2 Steel fibre reinforced concrete

As was mentioned above, a new material model for SFRC was developed as a user material law in ANSYS simulation software (2017). The material model has the form of the hyperbolic Drucker–Prager yield criterion (Jirasek and Bazant 2002)

$$f(\boldsymbol{\sigma}) = \alpha \frac{1}{3} I_1(\boldsymbol{\sigma}) + \sqrt{a^2 + 3J_2(\boldsymbol{\sigma})} - \sigma_y \tag{1}$$

where $\boldsymbol{\sigma}$ is a stress tensor, α is the pressure sensitivity coefficient, I_1 is the first invariant of the stress tensor, a is a material parameter, J_2 is the second invariant of the stress deviator tensor, and σ_y is the uniaxial yield stress. Material properties α and σ_y can be computed from the uniaxial compressive strength f_c and from the tensile strength f_t, as follows

$$\alpha = \frac{3\left(\sqrt{a^2 + f_c^2} - \sqrt{a^2 + f_t^2}\right)}{f_c + f_t} \tag{2}$$

$$\sigma_y = \frac{f_c\sqrt{a^2 + f_t^2} + f_t\sqrt{a^2 + f_c^2}}{f_c + f_t} \tag{3}$$

The evolution of the plastic strain $\dot{\boldsymbol{\varepsilon}}_{pl}$ is determined by the flow rule, as follows

$$\dot{\boldsymbol{\varepsilon}}_{pl} = \dot{\lambda} \frac{\partial q}{\partial \boldsymbol{\sigma}} \tag{4}$$

where parameter $\dot{\lambda} \geq 0$ is the rate of the plastic multiplier and q is the plastic potential. The Closest Point Projection (CPP) numerical method is used as a return mapping algorithm to the integration of the constitutive relations (Simo and Hughes 1998).

The softening function is trilinear, and can be determined with three uniaxial yield stresses $\sigma_{y,0}$, $\sigma_{y,1}$, $\sigma_{y,2}$ and three equivalent plastic strains $\varepsilon_{pl,eqv,1}$, $\varepsilon_{pl,eqv,2}$, $\varepsilon_{pl,eqv,3}$, see Fig. 4. Therefore, according to Eq. (3), the corresponding

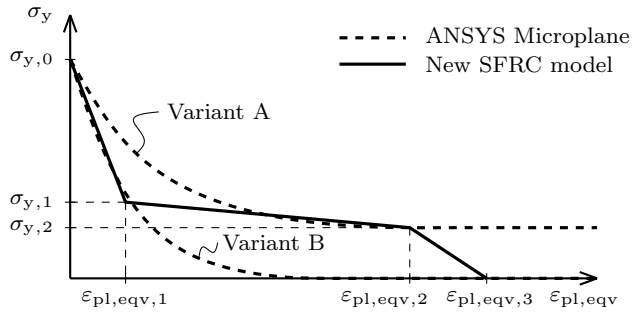

Fig. 4 Softening function for the Drucker–Prager material model

tensile strength values $f_{t,0}$, $f_{t,1}$, $f_{t,2}$ and the compressive strength value f_c have to be defined.

An advantage of the material model proposed here, in comparison with the ANSYS Microplane material model (ANSYS simulation software 2017) used in the preliminary study (Caldova et al. 2014a), lies in the advanced representation of the behaviour of SFRC in tension. The ANSYS Microplane model describes the behaviour in tension with exponential softening and residual strength. When the Microplane model approximates the behaviour of SFRC using residual strength (Variant A in Fig. 4), it is not possible to consider a complete failure of SFRC, and it is therefore not possible to predict the fire resistance of a structure. However, if SFRC is modelled with the Microplane material model with no residual strength (Variant B in Fig. 4), it is not possible to provide a sufficient representation of the ductile behaviour of SFRC in tension.

Material tests were performed to provide the necessary data for calibrating the SFRC material model. The mean material properties for the Drucker-Prager material model were determined on the basis of the results from the four-point bending tests at ambient temperature (20 °C) and at elevated temperatures (500 and 600 °C). Three four-point bending tests were performed at ambient temperature and six four-point bending tests were performed at elevated temperatures in 2010. The experimental program was later extended by three further tests at ambient temperature in 2012, see Table 1. Force-deflection curves were fitted as the average of the curves received from the measurements, see Fig. 5. The

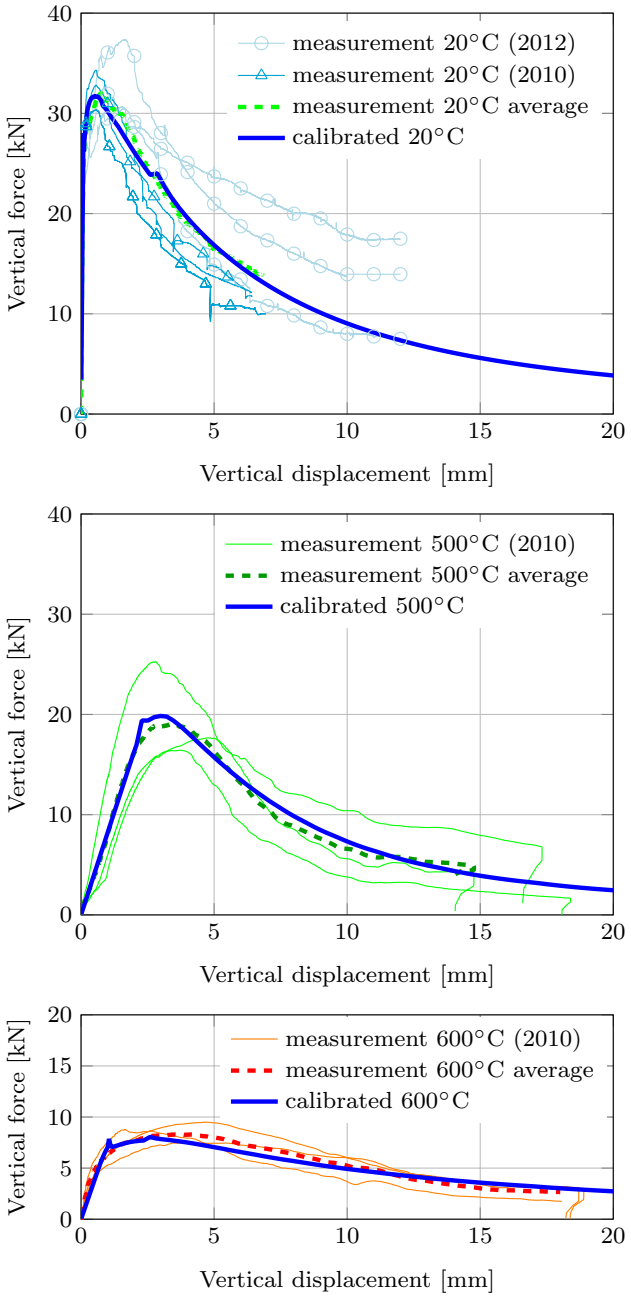

Fig. 5 Calibrated and measured force–deflection curves resulting from the four-point bending tests for ambient temperature (20 °C) and for elevated temperatures (500 and 600 °C)

Table 1 Overview of the number of four-point bending tests of SFRC at ambient and elevated temperatures

Temperature [°C]	Number of four-point bending tests realized in	
	2010	2012
20	3	3
500	3	0
600	3	0

calibrated stress–strain curves for different temperatures with the mean strength in tension are shown in Fig. 6.

For the FE model of the structure in Sect. 5, characteristic strength values are also needed. The values were defined according to EN 1990 (2002), as follows

$$X_d = m_X\left(1 - k_n V_X\right) \tag{5}$$

where m_X is the mean strength value, V_X is the coefficient of variation, and coefficient k_n for the 5% characteristic value

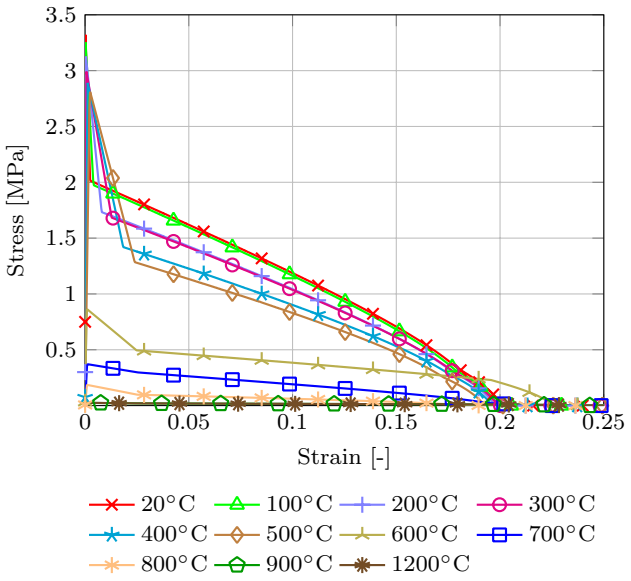

Fig. 6 Modelled stress–strain diagrams for tension with mean material properties of SFRC

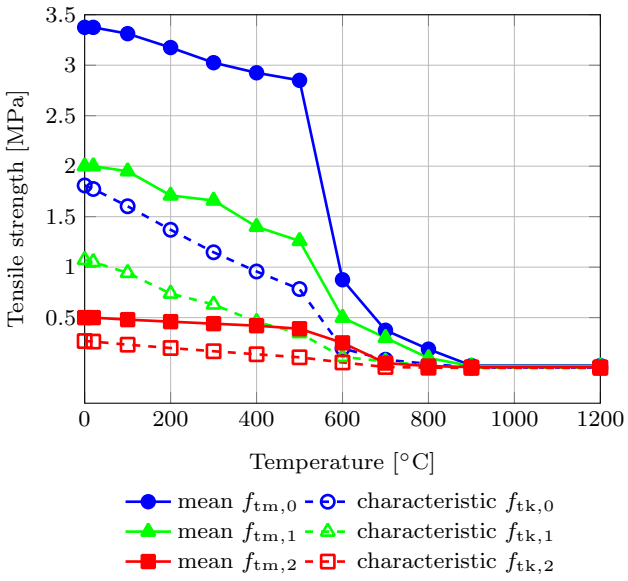

Fig. 7 Mean and characteristic tensile strength as a function of temperature

is defined according to the number of measurements. The variation coefficients and coefficients k_n were determined following the measurement outputs for ambient temperature (20 °C) and for elevated temperatures (500 and 600 °C). For tension, the products of coefficients V_X and k_n were linearly interpolated between temperatures of 20 and 600 °C, while for temperatures greater than 600° C a constant value was assumed. For compression, the products of coefficients V_X and k_n were assumed to have a constant value for all temperatures. The relationship between temperature and tension strength is shown in Fig. 7, and the relationship between temperature and compressive strength is shown in Fig. 8.

The thermal expansion for siliceous concrete was adopted for SFRC (EN 1992-1-2 2004).

3.3 Connectors

In a numerical model of timber fibre concrete composite structures, it is essential to have an appropriate model for the timber-SFRC coupling. The connection between the SFRC slab and the timber beams (GL24h) used for floor slab specimen ELE-1-120/160 is made of TCC 7.3 × 150 mm connectors with screws inclined 45° to the beam axis in two rows. The distance of the screws in one row was 100 mm. Push-out shear tests were performed to obtain the shear stiffness and the shear limit load of this connection. To determine the stiffness and the load bearing capacity in shear of the connection system, six push-out specimens at ambient temperature were tested, see Fig. 9.

The shear stiffness and the limit load of the connection are primarily determined by the strength of the connectors, the anchoring depths, and the strength of the base material. Friction effects between the connected parts take place only if their interfaces are compressed. A numerical model of the push-out shear tests was developed for calibrating the shear behaviour. The proposed model took into account the shear and tensile strength of the screws to be smeared over special bonded contact elements with a failure limit. The tangential contact stiffness and the limit tangential strength of the bonded contact are

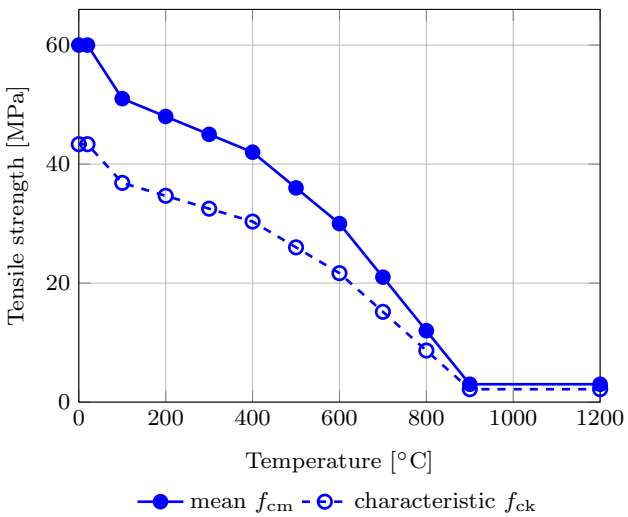

Fig. 8 Mean and characteristic compressive strength as a function of temperature

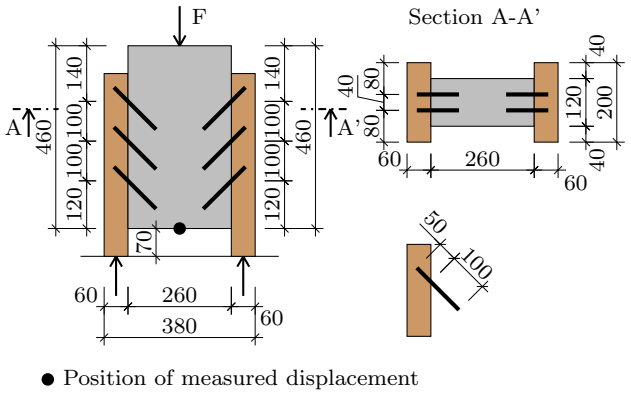

Fig. 9 Push-out shear test (Caldova et al. 2014b)

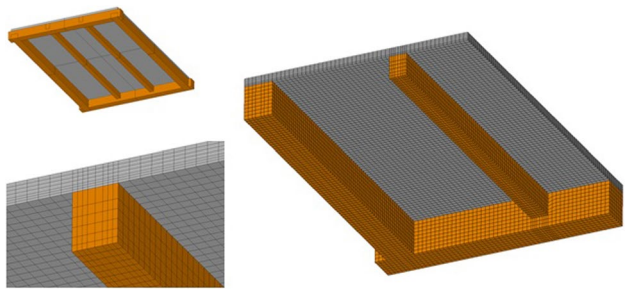

Fig. 10 FE mesh of a composite timber-SRFC floor (Caldova et al. 2014a)

defined by a bilinear function, which relates the tangential contact stress to the tangential slip distance (the relative tangent displacement on the contact surfaces). This bonded contact covers the middle part of the connection, where the screws are located. The rest of the connecting surfaces are covered by standard frictional contact. This type of model assumes failure of the screws only due to extensive straining of the screws and their rupture at contact surfaces between concrete and timber parts. This assumption corresponds to the results of the push-out shear tests, where this failure mode was observed for all specimens. Further details about the push-out shear tests and the numerical model can be found in Caldova et al. (2014b).

4 Verification of the FE model

The FE model was verified on the basis of the experimental results of the full-scale fire test on specimen ELE-1-120/160. The material properties of SFRC were obtained from the experimental compression tests and from four-point bending tests. The material properties of the connectors were obtained from the push-out shear tests, see Sects. 2 and 3.3. The FE model is therefore valid for the type of SFRC mixture, the connector and the timber class used here. The analysis was performed with ANSYS 15 FEM-based software (ANSYS simulation software 2017). The geometry was discretized with 3D solid elements, see Fig. 10. The model consists of one quarter of the whole structure, due to its double symmetry. A material model of the timber is described in Sect. 3.1. The screwed SFRC-timber connection was simulated applying contact elements (see Sect. 3.3). The analysis was performed as coupled thermo-mechanical with the one-way interaction coupling method.

4.1 Thermal analysis

The aim of the thermal analysis was to simulate the temperature field in the structure while it was being exposed to a standard fire. It was therefore performed as a nonlinear transient problem. The thermal material properties were obtained from EN 1992-1-2 (2004) for SFRC, and from EN 1995-1-2 (2004) for timber. The conductivity and the specific heat of SFRC and timber were modified on the basis of data from Lie and Kodur (1996), and were validated to the measured temperatures. Applied thermal material properties for SFRC and timber can be found in Caldova et al. (2014a). Convection and radiation were applied to the surfaces exposed to fire and to the ambient air. The numerical model was validated with a full-scale furnace experiment. Temperatures were measured in the centre of the slab in different positions, namely 40 mm and 20 mm from the bottom surface and at the unexposed (top) surface. Other measurements of temperatures were performed in the middle of the cross-section of the secondary timber beams in various positions along their length. For a comparison of the numerical and experimental output data, see Figs. 11 and 12.

4.2 Mechanical analysis

To determine the response of the structure during fire exposure and also the time of failure of the structure, an appropriate material model with plasticity was used for SFRC, see Sect. 3.2. The material properties of the SFRC and timber parts that define the strength and stiffness are generally dependent on temperature. It was assumed that the structure was deformed quite considerably before it collapsed (membrane state). The computations were therefore performed as being geometrically nonlinear. The structure is loaded by four forces, representing the weight of the concrete blocks used in the experiment, and further by the thermal strain resulting from the temperature field and the thermal expansion coefficients. The Newton–Raphson method (Belytschko et al. 2014) was chosen as a suitable method

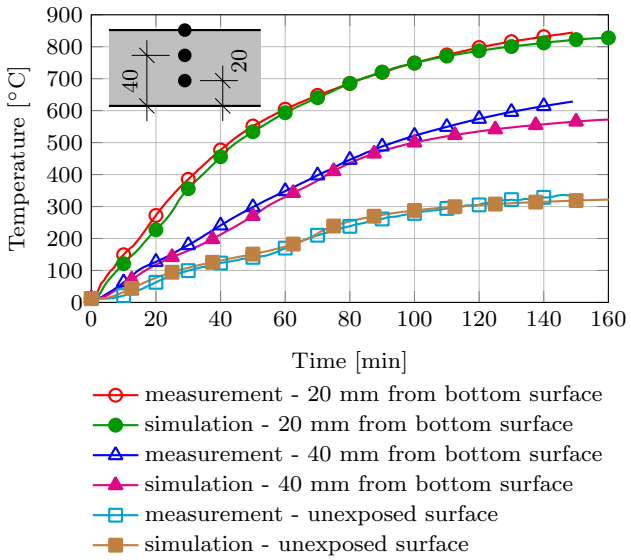

Fig. 11 Comparison of the temperatures in the centre of the SFRC slab resulting from numerical simulation and from experiment (Caldova et al. 2014a)

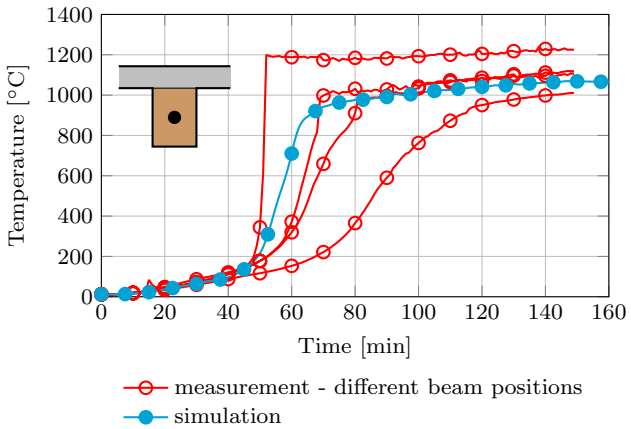

Fig. 12 Comparison of the temperatures in unprotected secondary timber beams resulting from numerical simulation and from experiment (Caldova et al. 2014a)

for solving a nonlinear problem of this kind. A sufficiently small time increment was selected to overcome convergence difficulties.

4.3 Predicting fire resistance on the basis of a numerical analysis

The time when the structure fails has to be properly determined by a numerical analysis to define the fire resistance of the structure. From a physical point of view, the failure of the structure occurs when static equilibrium is not reached. In the simulation, non-convergence occurs if the nonlinear algorithms cannot reach static equilibrium. However, non-convergence can also be caused by other effects, such as large load increments or material instability. Additional criteria have to be satisfied to prove that the reason for non-convergence is failure of the structure or of a part of the structure:

- A failure mode must be clearly seen, i.e. cracks which are shown as regions with high equivalent plastic deformation $\varepsilon_{\mathrm{pl,eqv,3}}$ (see Fig. 4).
- The regions with high Newton-Raphson residuals from equilibrium iterations must correspond with the failure mode. The Newton–Raphson residuals are unbalanced forces in the FE model in the non-converged state. They indicate regions where additional strength would be necessary to reach equilibrium.

The last converged step of the solution has to be used to evaluate the first of these two criteria. The second criterion can be verified in the iterations of the non-converged step. It is therefore recommended that very fine time steps be used, to come as close as possible to the non-converged state.

The criteria are applied partially on the basis of the experience and the judgment of analysts, because these two criteria cannot exactly quantify whether non-convergence occurs due to failure of the structure. However, if the FE model is properly built and verified, and if material models with failure are used, the simulation cannot overestimate the fire resistance indicated by non-convergence, as the static nonlinear analysis cannot find a state of equilibrium if rigid body motion occurs, indicating failure of the structure. However, the fire resistance can be underestimated due to non-convergence caused by other numerical problems, such as material instability or improper solver settings. Another option would be to use criteria based on controlling the maximal crack width or on controlling the deformations. As these criteria are not based on a comparison of stresses and strengths, or on a comparison of loads and resistances, they are not capable of predicting the true limit state.

A very widely used criterion for proving the failure of structures is a large change of the deflection rate (a large change in displacements for a small change in time/load). This effect is typical for stability problems. In the case of a floor slab, this is not observed before non-convergence of the simulation. This can be explained by extensive thermal damage to the SFRC slab in the membrane state, which leads abruptly to complete loss of load bearing capacity in the main crack, and the central part of the slab falls down. Such an abrupt change cannot be solved as a static problem. A transient nonlinear analysis would be needed to simulate this effect, which would be the best proof of failure. However, a transient simulation of the full-scale

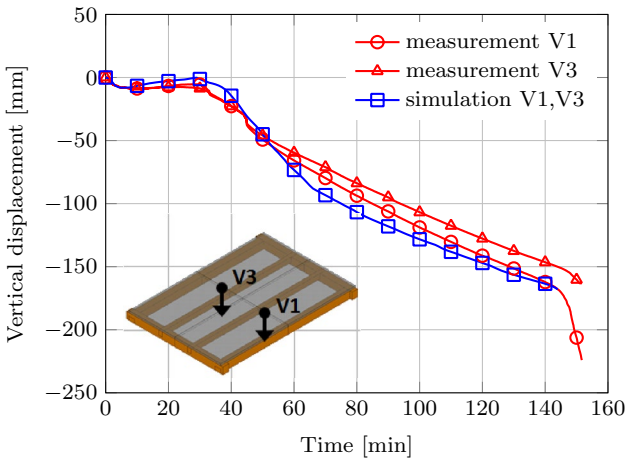

Fig. 13 Comparison of calculated and measured vertical displacements V1 and V3 on an SFRC slab

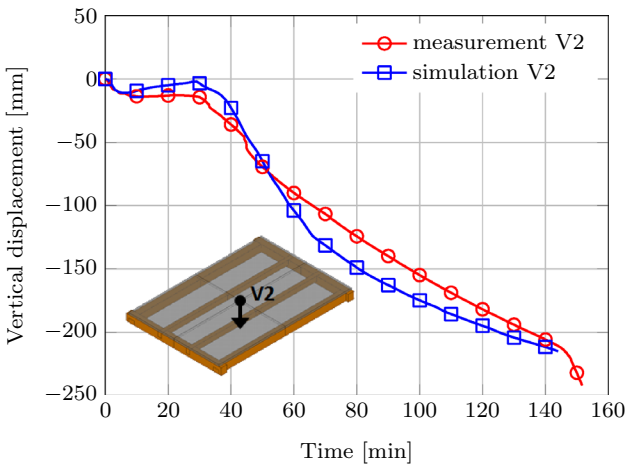

Fig. 14 Comparison of calculated and measured vertical displacements V2 on an SFRC slab

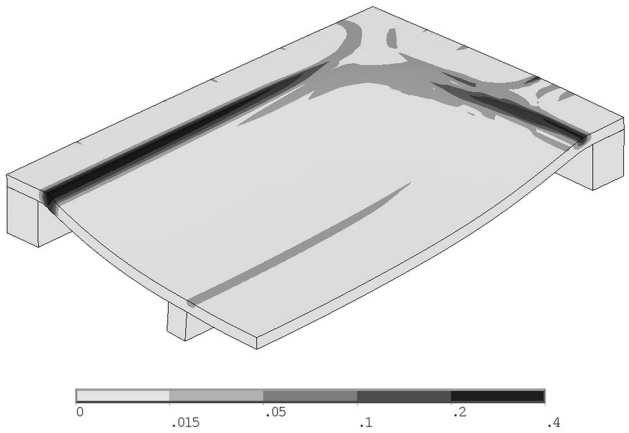

Fig. 15 Equivalent plastic strain $\epsilon_{pl,eqv}$ before collapse

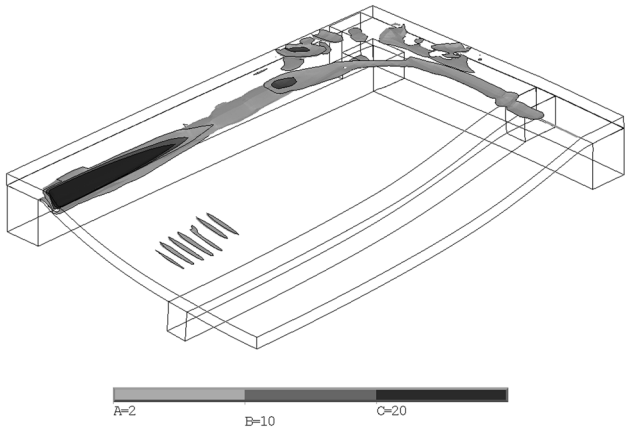

Fig. 16 Newton–Raphson residuals in the last non-converged step

furnace test would involve extensive calculation times, due to the very small time steps of the implicit or explicit time integration schema. The static nonlinear analysis can therefore be switched to a transient analysis at the last converged step of the static analysis to include inertia effects of the structure, which help to overcome convergence problems at time of the failure. This approach would be an important improvement to the current model, and will be tested in future research.

The results from the FE model and the full-scale furnace test were compared to validate the prediction quality of the FE model. The time history of the calculated vertical displacements was verified with measurements, see Figs. 13 and 14. Positions V1 to V3 are determined in Fig. 1. Position V2 is in the centre of the slab. The vertical displacements from the numerical analysis follow a similar trend to the measurements. The two results are comparable. Faster growth of the measured vertical displacements can be observed after 145 min, due to the beginning of structural failure. Non-convergence occurred in the numerical simulation at this time. To prove that this non-convergence was caused by failure of the structure, additional criteria mentioned above were verified. To check the failure mode, the equivalent plastic deformation $\epsilon_{pl,eqv,3}$ was evaluated in the SFRC slab, see Fig. 15. In the figure, there are two main cracks, which are situated along the timber frame. The equivalent plastic deformation exceeds a value of 0.2, indicating total loss of strength on a significant part of the crack. On the basis of these results, it can be stated that the collapse occurred due to further loss of load bearing capacity of the main crack, and the disjoining of the central part of the slab from the composite ring supported by the primary beams. The distribution of the Newton–Raphson residuals in Fig. 16 corresponds with

the failure mode indicated by the first criterion. Both of the criteria indicating failure of the structure were therefore satisfied in the simulation. The fire resistances predicted by the experiment and by the numerical simulation are comparable. The vertical displacements at the time of the structural failure and the failure modes are also equivalent. The agreement of the results from the experiment and from the numerical analysis proves that the defined criteria are correct, and that the numerical model is able to predict failure of the structure and to assess the fire resistance of the structure. The verified FE model can account for all possible failure modes of the SFRC slab. For the development of the FE model, it was not necessary to know the failure mode in advance and no special measures related to this mode were used. This statement is valid under the assumption that the failure mode occurs in the SFRC slab supported by the timber frame, and that the secondary beams are already burned. This is because the material model used for timber cannot simulate failure of the secondary beams. The current FE model is therefore not capable of predicting the load bearing capacity at ambient temperatures.

Mesh size dependence may occur due to the use of a material model with softening for the SFRC (Sect. 3.2). However, the numerical models for calibrating the material properties, for verifying the FE model, and also the FE models used for the analysis of several variants in Sect. 5 have the same mesh size. Mesh size dependence is therefore prevented.

The FE model validated to the experiments and described in this section can be further used for predicting the fire resistance of similar structures, see Sect. 5. Structures with different configurations, and structures with completely different dimensions or dispositions, have to be verified by additional experiments.

5 Fire resistance of timber steel fibre-reinforced concrete floor slabs

To determine the fire resistance, it is necessary to implement the semi-probabilistic safety concept of the Eurocode (EN 1992-1-2 2004) to the validated FE model. The validated FE model with mean material properties was therefore modified to an FE model with characteristic material properties, see Sect. 3.2. The FE model with mean material properties has shown that the membrane state of the SFRC slab is critical for the failure stage (Caldova et al. 2014b). Characteristic strengths were therefore applied only to SFRC.

A comparison of the vertical displacements in the middle of the slab from the measurements, the FE model with mean material properties and the FE model with characteristic material properties is shown in Fig. 17. The slab dimensions are 4.5×3.0 m^2. The slab is loaded with four forces with magnitude 6 kN, which represents a uniform load equal to 1.8 kN/m^2, see Table 2 (Design 2).

The FE models of the slabs with characteristic material properties were created in several variants differing in length and in load level. The slabs are 4.5, 5.0 and 6.0 m in length. They are 3 m in width. The loading of the slabs consists of four forces, as in the FE model with mean material properties. Their magnitudes are 5, 6 and 7 kN, which represent uniform loads, see Table 2. Thus there are a total of nine variants. The simulations were rather demanding in terms of the required computation time, so only nine variants were performed for the parametric study. The temperature loading was kept the same as for the FE model with mean material properties.

The aim of the analyses was to determine the fire resistance of the slabs. Fire resistance refers to the time for which a slab can withstand the fire without collapsing. The time development of the vertical displacements in the middle of the slab, marked as V2, for all variants, is shown in

Table 2 Fire resistance of the SFRC slab for various dimensions and loads

Design	Load during fire [kN]	Slab dimension [m] × [m]	Represented uniform load [kN/m^2]	Fire resistance [min]
1	$Q_{k,f} = 4 \times 5$	3×4.5	1.5	68
2[a]	$Q_{k,f} = 4 \times 6$	3×4.5	1.8	65
3	$Q_{k,f} = 4 \times 7$	3×4.5	2.1	64
4	$Q_{k,f} = 4 \times 5$	3×5.0	1.3	68
5	$Q_{k,f} = 4 \times 6$	3×5.0	1.6	66
6	$Q_{k,f} = 4 \times 7$	3×5.0	1.9	65
7	$Q_{k,f} = 4 \times 5$	3×6.0	1.1	85
8	$Q_{k,f} = 4 \times 6$	3×6.0	1.3	84
9	$Q_{k,f} = 4 \times 7$	3×6.0	1.6	82

[a]The full-scale furnace test was performed for this design

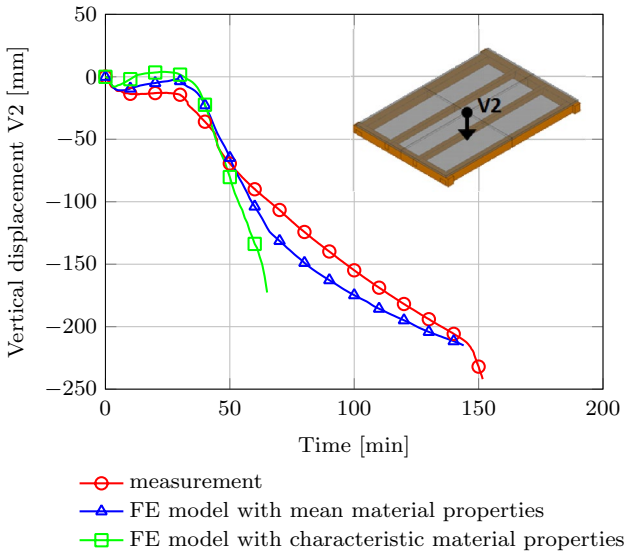

Fig. 17 Vertical displacements in the *middle* of the slab for measurements, the FE model with mean material properties, and the FE model with characteristic material properties (Design 2). The slab size is 4.5×3 m^2 and it is loaded with four forces with magnitude 6 kN

Fig. 18. From this figure, the fire resistance for all variants was determined as the time of structural failure. The results are presented in Table 2.

Observations can be drawn from comparison of the results from the FE model with mean material properties and the results from the FE model with characteristic material properties in Fig. 17. The models vary only in the mechanical material properties. However, the difference in the behaviour, for example the vertical displacement functions in Fig. 17, can be explained on the basis of understanding the behaviour of the slab. The behaviour was analysed with the FE model with mean material properties. Next, a simple description is provided. At the beginning of the fire process, there is a high thermal gradient across the SFRC slab. This causes high tension straining in the upper side of the SFRC slab. After the tensile strength of the SFRC has been reached, micro-cracking occurs. This reduces the stiffness of the slab. Micro-cracking occurs in an SFRC slab with characteristic material properties earlier than in an SFRC slab with mean material properties. This explains the upper hump of the vertical displacement function at the beginning of the analysis in the FE model with characteristic material properties in comparison with the FE model with mean material properties, see Fig. 17. In addition, after charring of the secondary beams the deflection later rises more quickly for the FE model with characteristic material properties, because the stiffness of the slab is lower. Finally the FE model with characteristic material properties reaches the membrane state, and collapses earlier than the FE model with mean material properties.

6 Conclusion

A finite element model (FE model) has been prepared for analysing SFRC floors with unprotected secondary glue laminated timber beams subjected to fire, taking tensile membrane action into account. The FE model was

Fig. 18 Vertical displacements in the *middle* of the slabs for nine FE models of the slabs

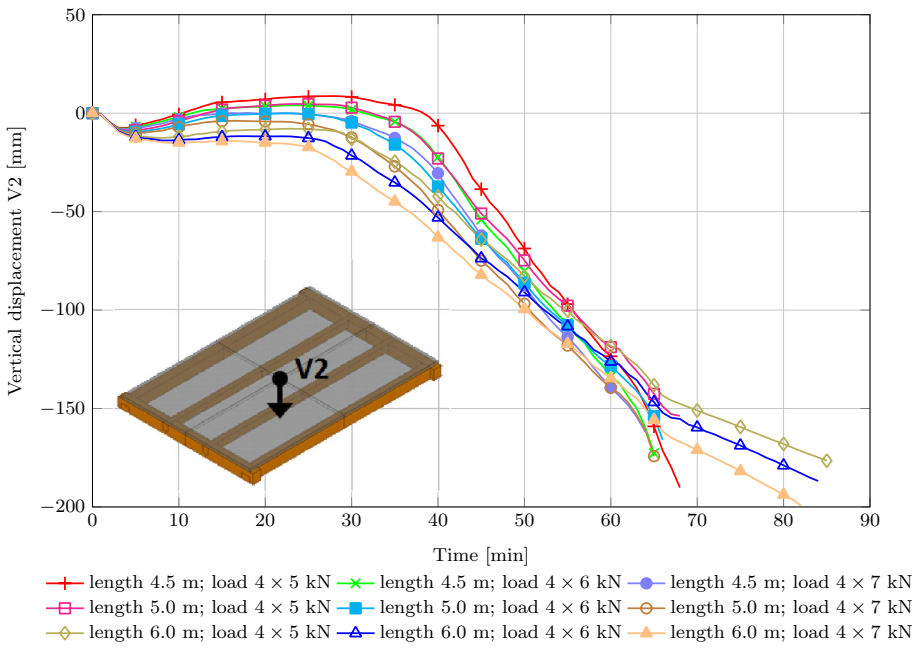

validated against the results from a full-scale furnace test. The FE model takes into account geometric and material nonlinearity, mechanical damage due to thermal loading, and a nonlinear model of the connection between the SFRC slab and the timber beams. The new material model has been created to improve the simulated behaviour in tension of SFRC. The semi-probabilistic safety concept of the Eurocode was also applied to the FE model. This FE model was used for calculating the fire resistance of several variants of timber steel fibre reinforced concrete floor slabs for different span lengths and load levels. This parametric study shows that the FE model validated on a full-scale fire test can help to assess structures similar to the tested structures. The results from the calculations contribute to the safe and efficient use of membrane action for the design of composite slab systems subjected to fire. This approach will be used for creating a catalogue which will define the fire resistance for specific parameters of the structure, for example dimensions, loads and materials.

The finite element based approach for analysing and assessing composite SFRC-timber floors subjected to fire could provide an alternative to analytical models. However, no analytical models for structures of these types have yet been developed, due to the need to make significantly simplified assumptions. For example, for many analytical models it is necessary to know the failure mode of the structure. However, FE models are easier to develop and can take into account physical phenomena related to a thermo-mechanical analysis, such as the transient heat flow in the structure, geometrical nonlinearity, and thermal and mechanical damage due to fire loading. However, FE models need many material tests to obtain the material properties, which are often nonlinear and temperature-dependent. Due to the complexity of such FE models, full-scale furnace tests are needed for validation.

The validated FE model was able to predict the failure mode observed in the full-scale test and the same fire resistance as in the experiment. This proves that for the FE model it is not necessary to know the failure mode in advance, because no special measures related to this particular mode were used. There are still some limits and disadvantages. For example, the mesh dependency and the criteria indicating failure of the structure need to be further analysed and improved. In addition, the FE model should be validated with other full-scale tests and verified against other models of other types of SFRC-timber floors.

Acknowledgements This work has been supported by the Ministry of Education, Youth and Sports within National Sustainability Programme I, Project no. LO1605, and by the Grant Agency of the Czech Republic, within the framework of Project No. 15-19073S.

References

ANSYS simulation software (2017) Ansys Inc., Pennsylvania, USA

Bailey CG (2004) Membrane action of slab/beam composite floor systems in fire. Eng Struct 26(12):1691–1703

Bednar J, Wald F, Vodicka J, Kohoutkova A (2012) Membrane action of composite steel fibre concrete slab in fire. Proc Eng 40:498–503

Belytschko T, Liu WK, Moran B, Elkhodary KI (2014) Nonlinear finite elements for continua and structures. Wiley, p 804. ISBN: 978-1-118-63270-3

Caldova E, Vymlatil P, Wald F, Kuklikova A (2014a) Timber steel fiber reinforced concrete floor slabs in fire: experimental and numerical modeling. J Struct Eng

Caldova E, Blesak L, Wald F, Kloiber M, Uruschdze S, Vymlatil P (2014b) Behaviour of timber and steel fibre reinforced concrete composite constructions with screwed connections. Wood Res 59(4):639–660

Ceccotti A (2002) Composite concrete-timber structures. Prog Struct Eng Mater 4(3):264–275

EN 1990 (2002) Eurocode: basis of structural design. CEN, Brussels

EN 1992-1-2 (2004) Eurocode 2: design of concrete structures—Part 1–2: General rules—structural fire design. CEN, Brussels

EN 1995-1-1 (2004) Eurocode 5: design of timber structures Part 1-1: General Common rules and rules for buildings. CEN, Brussels

EN 1995-1-2 (2004) Eurocode 5: Design of timber structures—Part 1–2: General—structural fire design. CEN, Brussels

Fontana M, Frangi A (2000) Fire behaviour of timber-concrete composite slabs. Fire Saf Sci 6:891–902

Frangi A, Fontana M (2003) Thermal expansion of wood and timber-concrete composite members under Iso-fire exposure. Fire Saf Sci 7:1111–1122

Frangi A, Knobloch M, Fontana M (2009) Fire design of timber-concrete composite slabs with screwed connections. J Struct Eng 136(2):219–228

Holschemacher K, Klotz S, Weise D (2002) Application of steel fibre reinforced concrete for timber-concrete composite constructions. Lacer 7:161–170

Jirasek M, Bazant Z (2002) Inelastic analysis of structures. Wiley, p 758. ISBN: 978-0-471-98716-1

Lie TT, Kodur VK (1996) Thermal and mechanical properties of steel-fibre-reinforced concrete at elevated temperatures. Can J Civ Eng 23:511–517

Lim L (2003) Membrane action in fire exposed concrete floor systems (Doctoral dissertation) (**ISSN 1173-5996**)

Simo JC, Hughes TJR (1998) Computational inelasticity. Springer-Verlag, New York. p 392. ISBN: 0-387-97520-9

Stojić D, Cvetković R (2001) Analysis of a composite timber-concrete structures according to the limit states: design and innovative methods in coupling of a timber and concrete. Facta Univ Ser Arch Civ Eng 2(3):169–184